

## Redesign of Carnitine Acetyltransferase Specificity by Protein Engineering\*

Received for publication, March 9, 2004, and in revised form, May 18, 2004  
Published, JBC Papers in Press, May 21, 2004, DOI 10.1074/jbc.M402685200

Antonio G. Cordente<sup>‡§</sup>, Eduardo López-Viñas<sup>¶</sup>, María Irene Vázquez<sup>‡\*\*</sup>, Jan H. Swiegers<sup>‡‡</sup>,  
Isak S. Pretorius<sup>‡‡</sup>, Paulino Gómez-Puertas<sup>¶</sup>, Fausto G. Hegardt<sup>‡§§</sup>, Guillermina Asins<sup>‡</sup>,  
and Dolors Serra<sup>‡</sup>

From the <sup>‡</sup>Department of Biochemistry and Molecular Biology, School of Pharmacy, University of Barcelona, Diagonal 643, E-08028 Barcelona, Spain, <sup>¶</sup>Bioinformatics Laboratory (Centro de Astrobiología/Consejo Superior de Investigaciones Científicas), Torrejón de Ardoz, E-28850 Madrid, Spain, and <sup>‡‡</sup>The Australian Wine Research Institute, P. O. Box 197, Glen Osmond, Adelaide SA-5064, Australia

In eukaryotes, L-carnitine is involved in energy metabolism by facilitating  $\beta$ -oxidation of fatty acids. Carnitine acetyltransferases (CrAT) catalyze the reversible conversion of acetyl-CoA and carnitine to acetylcarnitine and free CoA. To redesign the specificity of rat CrAT toward its substrates, we mutated Met<sup>564</sup>. The M564G mutated CrAT showed higher activity toward longer chain acyl-CoAs: activity toward myristoyl-CoA was 1250-fold higher than that of the wild-type CrAT, and lower activity toward its natural substrate, acetyl-CoA. Kinetic constants of the mutant CrAT showed modification in favor of longer acyl-CoAs as substrates. In the reverse case, mutation of the orthologous glycine (Gly<sup>553</sup>) to methionine in carnitine octanoyltransferase (COT) decreased activity toward its natural substrates, medium- and long-chain acyl-CoAs, and increased activity toward short-chain acyl-CoAs. Another CrAT mutant, M564A, was prepared and tested in the same way, with similar results. We conclude that Met<sup>564</sup> blocks the entry of medium- and long-chain acyl-CoAs to the catalytic site of CrAT. Three-dimensional models of wild-type and mutated CrAT and COT support this hypothesis. We show for the first time that a single amino acid is able to determine the substrate specificity of CrAT and COT.

Carnitine acyltransferases are essential for the  $\beta$ -oxidation of fatty acids and thus play an important role in energy metabolism in eukaryotes. There are three carnitine acyltrans-

ferase families: the carnitine palmitoyltransferases (CPTs)<sup>1</sup>, CPT I and CPT II, are essential for mitochondrial  $\beta$ -oxidation and are located in the outer and inner mitochondrial membrane, respectively. CPT I facilitates the transfer of long-chain fatty acids from the cytoplasm to the mitochondrial matrix, which is the rate-limiting step in  $\beta$ -oxidation (1). Mammalian tissues express three isoforms of CPT I (each encoded by a different gene), in liver (L-CPT I), muscle (M-CPT I) and brain (CPTI-c) (2–4). Carnitine octanoyltransferase (COT) facilitates the transport of medium-chain fatty acids from peroxisomes to mitochondria through the conversion of acyl-CoAs, shortened by peroxisomal  $\beta$ -oxidation, into acetylcarnitine (5). Carnitine acetyltransferase (CrAT) catalyzes the reversible conversion of acetyl-CoA and carnitine to acetylcarnitine and free CoA.

Due to the impermeability of organelle membranes to CoA, CrATs function in a compartmental buffering system by maintaining the appropriate levels of acetyl-CoA and CoA in cellular compartments. In peroxisomes they remove excess activated acetyl groups releasing free CoA, which can then accept more acetyl groups produced by  $\beta$ -oxidation, thereby allowing the oxidation to proceed. This indirectly facilitates the transport of acetyl moieties to the mitochondria for oxidation (6, 7). Mitochondrial CrAT plays a major role in modulating matrix acetyl-CoA concentration. The production and utilization of acetyl-CoA in the mitochondrial matrix lie at a major metabolic crossroads. Regulation of the fate of acetyl-CoA is mediated, to a large extent, by the effects of the molecule itself on pyruvate dehydrogenase kinase, which is inhibited by a high acetyl-CoA/CoA ratio. In the liver, mitochondrial acetyl-CoA also activates the key gluconeogenic enzyme pyruvate carboxylase. Therefore, high rates of  $\beta$ -oxidation of fatty acids result in the activation of gluconeogenesis from pyruvate and its precursors. In mammalian tissues, CrATs can also contribute to the excretion of excess or harmful acyl molecules, such as acetylcarnitines. CrAT activity has also been implicated in the cell cycle from G<sub>1</sub> to S phase (8). CrATs also appear to play an important role in human health. For example, decreases in CrAT activity have been reported in patients with disorders of the nervous system, such as Alzheimer's disease (9, 10), ataxic encephalopathy (11), and several vascular diseases (12, 13).

The crystal structures of the mouse and human CrAT have recently been reported, alone and complexed with their substrates carnitine or CoA (14, 15). The data provide critical insights into the molecular basis for acyl-chain transfer and a

\* This study was supported in part by Grants BMC2001-3048 from the Dirección General de Investigación Científica y Técnica, by Grant C3/08 from the Fondo de Investigación Sanitaria of the Instituto de Salud Carlos III, Red de Centros en Metabolismo y Nutrición from the Ministry of Health, Madrid, Spain, by the Ajut de Suport als Grups de Recerca de Catalunya (2001SGR-00129), Spain, and by a grant from the Fundación Ramón Areces. The costs of publication of this article were defrayed in part by the payment of page charges. This article must therefore be hereby marked "advertisement" in accordance with 18 U.S.C. Section 1734 solely to indicate this fact.

The atomic coordinates and structure factors (codes 1NMS and INDB) have been deposited in the Protein Data Bank, Research Collaboratory for Structural Bioinformatics, Rutgers University, New Brunswick, NJ (<http://www.rcsb.org/>).

The nucleotide sequence(s) reported in this paper has been submitted to the GenBank™/EBI Data Bank with accession number(s) AJ620886.

§ Recipient of a fellowship from the Generalitat de Catalunya.

¶ Recipient of a fellowship from the Fundación Ramón Areces.

\*\* Recipient of a fellowship from the Ministry of Science and Technology.

§§ To whom correspondence should be addressed. Tel.: 34-93-402-4523; Fax: 34-93-402-4520; E-mail: fgarciaheg@ub.edu.

<sup>1</sup> The abbreviations used are: CPT, carnitine palmitoyltransferase; COT, carnitine octanoyltransferase; CrAT, carnitine acetyltransferase; wt, wild-type; nt, nucleotide(s); GST, glutathione S-transferase.

possible common mechanism for all carnitine acyltransferases. A histidine residue interacts with an aspartic/glutamic acid at the catalytic site (16) and acts as a general base (1). The position of this histidine at the center of the catalytic tunnel allows access to both substrates carnitine and acetyl-CoA, which lie on opposite sides of the tunnel (15, 17). The catalytic His extracts the proton from the 3-hydroxyl group of carnitine or the thiol group of CoA, depending on the direction of the reaction. The activated hydroxyl or thiol group then has direct access to the carbonyl carbon in acyl-CoA or acylcarnitine, and the reaction proceeds without the formation of an acyl-enzyme intermediate (14). Previous site-directed mutagenesis experiments have demonstrated an essential catalytic role for the homologous histidines in CPT II, L-CPT I, and COT (16, 18, 19).

Substrate specificity of carnitine acyltransferases may be a function of structural features that govern the fit of the carbon chain. The acetyl group of acetylcarnitine points toward a hydrophobic pocket in the CrAT crystal, which is located at the intersection of the two beta sheets in the enzyme (14). In CrAT, this pocket is partly occupied by the side chain of Met<sup>564</sup>. Because the equivalent residue in all other carnitine acyltransferases is a glycine, Met<sup>564</sup> could be the residue that blocks the access of medium- and long-chain fatty acids to the hydrophobic pocket.

Here we report site-directed mutagenesis that modified CrAT Met<sup>564</sup> to glycine, its counterpart in COT, CPT I and CPT II. We assessed the kinetic properties of the yeast-expressed mutant for acyl-CoA substrates other than acetyl-CoA. Catalytic efficiency and enzyme activity of the mutant favored longer acyl-CoAs. Moreover, we also mutated COT Gly<sup>553</sup> (orthologous to CrAT Met<sup>564</sup>) to methionine. The activity of the COT mutant G553M toward several acyl-CoAs was practically identical to wt CrAT. Docking analyses on the three-dimensional models of wt and mutated CrAT and COT confirm that Met<sup>564</sup> blocks the entry of the hydrocarbon chain of acyl-CoAs to the CrAT molecule.

#### EXPERIMENTAL PROCEDURES

**Cloning of Rat CrAT**—Rat CrAT cDNA was amplified by PCR, using the *PfuTurbo*® DNA polymerase (Stratagene), from rat testis cDNAs using two primers: CrATATG.for (5'-ATGTTAGCTTTTGCTGCCAG-3') and CrAT2100.rev (5'-CTTGTTTCAGCCTCTGGGCTCAGC-3'). The former was taken from a rat CrAT DNA sequence (XM\_242301) and contains the ATG start codon, and the latter was designed from a rat cDNA clone that corresponds to the 3'-untranslated region of rat CrAT (GenBank AA925306). A fragment of 2070 nucleotides was obtained, purified, and subcloned into the pGEM®-T vector (Promega), yielding the pGEM-T-CrAT<sup>wt</sup> construct. The rat CrAT cDNA fragment was sequenced (GenBank AJ620886) with an Applied Biosystems 373 automated DNA sequencer.

**Construction of the Rat CrAT and COT Models**—The structural models for wt CrAT and wt COT were constructed using homology modeling procedures based on the multiple, structure-based alignment of the rat CrAT and COT amino acid sequences with members of the carnitine acyltransferase family, including the three-dimensional structures of human CrAT (Protein Data Bank (PDB) entry 1NMS (15)) and mouse CrAT (free enzyme structure: PDB accession number 1NDB; carnitine complex: 1NDF; CoA complex: 1NDI (14)). The three-dimensional models were built using the program Swiss-Pdb Viewer and the SWISS-MODEL server facilities (20–23) (available at www.expasy.ch/swissmod/SWISS-MODEL.html). The structural quality was checked using the WHAT-CHECK routines (24) from the WHAT IF program (25) and the PROCHECK validation program from the SWISS-MODEL server facilities (26); briefly, the quality values of both models are within the range expected for protein structural models. The three-dimensional models of CrAT mutants M564G and M564A and COT mutant G553M were built by the same procedures using the structures obtained for the respective wt enzymes as templates.

**Molecular Docking**—Docking calculations to obtain a molecular model of the interaction between the substrates acetyl-CoA, decanoyl-CoA, and myristoyl-CoA and the three-dimensional models of the pu-

tative receptor proteins wt CrAT, wt COT, CrAT M564G, M564A, and COT G553M were performed using the programs Autodock (27, 28) and Hex (29). Protein targets and ligands (acyl-CoAs and carnitine) were prepared using the algorithms Addsol and Autotors from the Autodock package. For each individual calculation, a global search (100 cycles) was performed using Autogrid and Autodock. Having discarded the non-realistic positions far from the substrate cavity described for acetyl-CoA in the PDB 1NDI crystal structure, the ligand positions of lowest energy were selected. The relative positions of the acyl extensions of the ligand molecules were refined using the rigid docking program Hex.

**Construction of Plasmids For Expression in *Saccharomyces cerevisiae***—For expression experiments on CrAT, the 1925-nt fragment containing the rat CrAT coding region was subcloned into the *S. cerevisiae* expression plasmid pYES2 (Invitrogen). To enable cloning into the only HindIII site of the pYES2 plasmid, a HindIII site (underlined in the HindIII-CrAT.for primer) immediately 5' of the ATG start codon was introduced by PCR, using pGEM-T-CrAT<sup>wt</sup> as template. A consensus sequence (in boldface type), optimized for efficient translation into yeast, was also introduced in the same PCR, using the forward primer HindIII-CrAT.for (5'-TCGATAAGCTTATAAAAATGTTAGCCTTTGCTGCCAGAAC-3') and the reverse primer EcoRICrAT.rev (5'-CGGAAT-TCCGCCAAAGTGGGCTTGGCTGTG-3'), which introduces a HindIII and EcoRI sites (underlined). PCR products were digested with HindIII and EcoRI and ligated to the pYES2 plasmid, producing pYESCrAT<sup>wt</sup>. For protein expression experiments on COT, plasmid pYESCOT<sup>wt</sup> was prepared as described elsewhere (19).

**Construction of Plasmids for Expression in *Escherichia coli***—To express the rat CrAT protein in *E. coli*, a cDNA fragment containing CrAT was obtained from plasmid pYESCrAT<sup>wt</sup>, digested with HindIII, blunt-ended, and again digested with EcoRI. This fragment was then purified and subcloned into the expression vector pGEX-6P-1 previously digested with BamHI, blunt-ended, and again digested with EcoRI. The plasmid obtained was pGEX-CrAT<sup>wt</sup>.

**Construction of Site-directed Mutants**—CrAT mutants M564G, M564A, H343A, and E347A were constructed using the QuikChange PCR-based mutagenesis procedure (Stratagene) with the pYESCrAT<sup>wt</sup> plasmid as template. COT mutant G553M was constructed using pYESCOT<sup>wt</sup> as template. The following primers were used: primer CrAT-M564G.for (5'-CAAGACAGACTGTGTCGGGTCCTTCGGACCTGTG-3'), and primer CrATM564G.rev (5'-CACAGGTCCGAAGGACCCGACACAGTCTGTCTTG-3') were used to construct pYESCrAT<sup>M564G</sup>; primer CrATM564A.for (5'-CAAGACAGACTGTGTCGGGTCCTTCGGACCTGTG-3'), and primer CrATM564A.rev (5'-CACAGGTCCGAAGGACCCGACACAGTCTGTCTTG-3') were used to construct pYESCrAT<sup>M564A</sup>; primer CrATH343A.for (5'-GTGGGATGGTTTATGAAGCTGCAGCTGCAGAAGCG-3'), and primer CrATH343A.rev (5'-CCCTTCTGCAGCTGCAGCTTCATAAACCATCCAC-3') were used to construct pYESCrAT<sup>H343A</sup>; primer CrATE347A.for (5'-GAACATGCAGCTGCAGCAGGGCCCCCAATTGTC-3') and primer CrATE347A.rev (5'-GACAATGGGGGGCCCTGCTGCAGCTGCATGTTC-3') were used to construct pYESCrAT<sup>E347A</sup>; primer COTG553M.for (5'-GTTACTTACGAATTCAGATGGTCTGGTTCCCATG-3'), and primer COTG553M.rev (5'-CATGGGAACCACGACC-ATCTGAATTCGTAAGTAAC-3') were used to construct pYESCOT<sup>G553M</sup>. In all the cases the mutated nucleotides are underlined. The appropriate substitutions, as well as the absence of unwanted mutations, were confirmed by sequencing the inserts.

**Expression of CrAT and COT in *S. cerevisiae***—The plasmids containing wt and mutants CrAT and COT were expressed in yeast cells, and mitochondrial and peroxisomal cell extracts were prepared as previously described (18, 19). A strain of *S. cerevisiae* devoid of COT activity and lacking the endogenous *CAT2* gene (FY23 $\Delta$ cat2 (*MATa* *trp1 ura3*  $\Delta$ cat2::LEU2)) was used as an expression system. Although this strain conserves two additional CrAT genes (*YAT1* and *YAT2*) (30), its carnitine acetyltransferase activity in the conditions in which it was expressed was not detected.

**Expression and Purification of Rat CrAT Wild-type in *E. coli***—For expression and purification of rat CrAT protein the glutathione *S*-transferase (GST) gene fusion system (Amersham Biosciences) was used. The construction pGEX-CrAT<sup>wt</sup> was transformed into *E. coli* BL21, and fusion protein GST-CrAT was overexpressed overnight after the addition of 0.1 mM isopropyl-1-thio- $\beta$ -D-galactopyranoside at 18 °C. The soluble fusion protein was purified from bacterial lysates using glutathione-Sepharose 4B with a batch method. Finally, CrAT was eluted by cleavage of the fusion protein with the site-specific protease PreScission protease (Amersham Biosciences). Purity of rat CrAT protein was checked by SDS-PAGE.

**Determination of Carnitine Acyltransferase Activity**—Carnitine acyltransferase activity was measured by a slight modification of an end

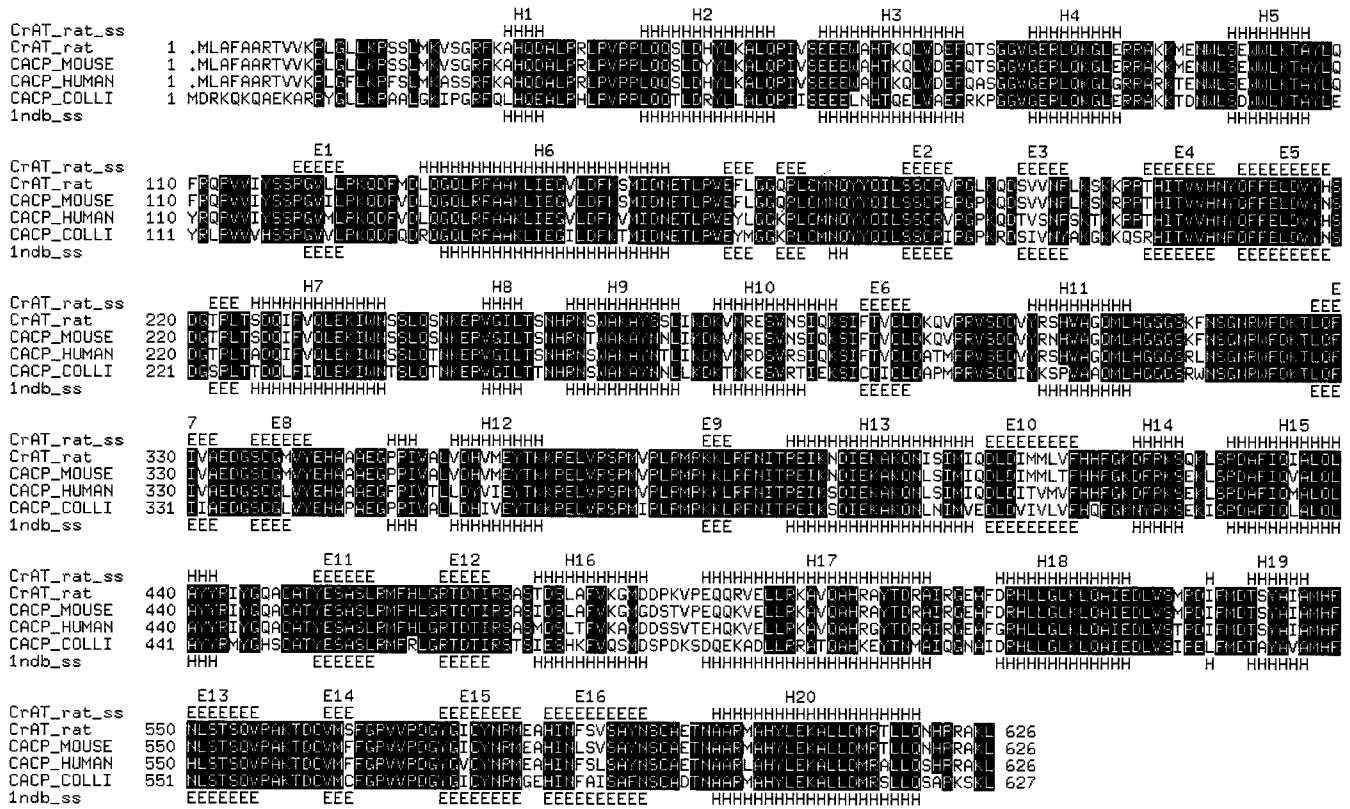


FIG. 1. Sequence and proposed secondary structure of rat carnitine acetyltransferase (CrAT). Alignment of amino acid sequence of carnitine acetyltransferases from rat (*CrAT-rat*), mouse (Swiss-Prot code: *CACP\_MOUSE*), human (*CACP\_HUMAN*), and domestic pigeon, *Columba livia* (*CACP\_COLL1*). The secondary structure elements for Protein Data Bank entry 1NDB (mouse carnitine acetyltransferase) are numbered as previously published (14). The modeled secondary elements for rat CrAT are also indicated (H: alpha helix; E: beta strand). Residues are shaded according to conservation.

point fluorometric method (31). The assay was conducted for 8 min at 30 °C in a solution containing 0.1 mM acyl-CoA, 1.5 mM EDTA, 1.5 mM L-carnitine, 40 mM HEPES buffer (pH 7.8) in a total volume of 600 µl. Reactions were started by the addition of yeast-expressed protein: 5 µg for CrAT, 4 µg for COT, or from 0.1 to 5 µg of *E. coli*-expressed CrAT. Parallel (blank) assays were run in the absence of L-carnitine. Reactions were arrested by heat treatment (10 min at 70 °C). Proteins were sedimented by centrifugation for 10 min at 13,400 × g; 550 µl of the supernatant was collected, 35 µl of a stock solution (2 mg/ml) of 7-fluoro-2,1,3-benzoxadiazole-4-sulfonamide was added, and the mixture was incubated at 50 °C for 30 min. Fluorescence intensities, indicative of the binding of the CoA thiol group to 7-fluoro-2,1,3-benzoxadiazole-4-sulfonamide, were measured in 10-mm path-length glass cuvettes (700 µl) at 391 nm (excitation wavelength) and 515 nm (emission wavelength). These fluorescence intensities were compared with a standard curve for CoA between 0 and 30 nmol. All fluorometer recordings were performed with a PerkinElmer Life Sciences LS 45 luminescence spectrometer, and the enzyme activities were measured in duplicate. For determination of the  $K_m$  for carnitine, acyl-CoA was fixed at 0.1 mM. For determination of the  $K_m$  for acyl-CoA, carnitine concentration was fixed at 1.5 mM. Values reported are the means and standard deviations of three or four determinations. All protein concentrations were measured using the Bio-Rad protein assay with bovine albumin as standard.  $K_m$  and  $V_{max}$  values were calculated with the analysis of variance program.

**Generation of Anti-rat Carnitine Acetyltransferase Antibodies**—Two female New Zealand White rabbits were each injected subcutaneously on days 0, 21, 42, and 63 with 150 µg of the purified CrAT protein. The protein was emulsified 1:1 with Freund's complete adjuvant (day 0) or incomplete adjuvant (days 21, 42, and 63) in a total volume of 1 ml. Rabbits were bled completely 10 days after the third booster (day 73), and then the serum with the anti-rat CrAT antibodies was isolated. All the procedures were performed in accordance with the recommendations of the Animal Experimentation Ethical Committee of the University of Barcelona.

**Immunological Techniques**—*S. cerevisiae* protein extracts (8 µg for CrAT and 10 µg for COT) were treated with sample buffer and subjected to 8% SDS-PAGE. Electroblothing to nitrocellulose sheets was

carried out for 1 h at 250 mA. Immunodetection of CrAT was performed using anti-CrAT antibodies (1:10,000 dilution), and immunodetection of COT was done with anti-COT antibodies obtained as described elsewhere (19). The blots were developed with the ECF Western blotting system from Amersham Biosciences. The quantifications were carried out using a fluorescence scanning device from Molecular Dynamics Storm 840™.

RESULTS

**Isolation of Rat CrAT**—A cDNA fragment corresponding to rat CrAT was isolated from rat testis mRNA by RT-PCR and sequenced. The sequence has been deposited in the GenBank™ (accession no. AJ620886).

Rat CrAT mRNA encodes a predicted protein of 626 amino acids with a molecular mass of 70,800 Da (Fig. 1), which shows 96 and 90% identity with CrAT from mouse and human, respectively. The N-terminal end of the primary translation product has a sequence of 21 amino acids before the second methionine, which is the putative first amino acid in peroxisomal CrAT. By comparison with other CrATs we postulated a 29-amino acid sequence that transports the protein into mitochondria (32). Its amino acid composition is consistent with the general composition given for leader peptides that translocate cytosolic synthesized proteins into mitochondria (33).

**Re-engineering CrAT Substrate Specificity**—Inspection of the published crystal structure of CrAT revealed that acetyl-CoA points to a hydrophobic pocket at the intersection of two β-sheets (strands β1 and β8 in the N domain and strands β13 and β14 in the C domain) and helix α12 (14). This pocket is partially occupied by the side chain of Met<sup>664</sup> from strand β14. Because this methionine is only present in CrAT, but not in other carnitine acyltransferases (CPT I, CPT II, or COT) (Fig. 2), in which the equivalent residue is a glycine, we hypothesized that it could play a role in the correct positioning of the

CPT1_RAT	252	SNYYAMEML	469	INAEHSWADAPIVGHILWEYVMATDVF	683	RLSTSQTPOQQVELDFEKNPDYVSCGSGFGPVA
CPT1_MOUSE	252	SNYYAMEML	469	INAEHSWADAPIVGHILWEYVMATDVF	683	RLSTSQTPOQQVELDFEKNPDYVSCGSGFGPVA
CPT1_HUMAN	252	SNYYAMDLL	469	INAEHSWADAQIVAHILWEYVMSIDSL	683	RLSTSQTPOQQVELDFLENNPEYVSSGSGFGPVA
CPTM_HUMAN	254	SNYYVMDLV	469	INAEHSWADAPIIGHILWEFVLGTDSTF	683	RLSTSQTPOQQVELDFEKNPDYVSCGSGFGPVA
CPTM_RAT	254	SNYYAMDVF	469	INTEHSWADAPIIGHILWEFVLATDTF	683	SLSTSQTPOQQVELDFEKNPDYVSCGSGFGPVA
CPTM_MOUSE	254	SNYYAMDVF	469	INTEHSWADAPIIGHILWEFVLATDTF	683	SLSTSQTPOQQVELDFEKNPDYVSCGSGFGPVA
CPTC_MOUSE	251	STYYMDFL	465	LSVEHSWADCPVSGHLMWEFTLATECF	678	LLSTSQVPPVQQTHLIDVHNYPDYVSSGSGFGPAD
CPTC_HUMAN	252	SNYYMDFL	466	LSVEHSWADCPISGHLMWEFTLATECF	680	QLSTSQTIPVQQMHLFDVHNYPDYVSSGSGFGPAD
CPT2_RAT	131	FNPFMAFNP	368	VHFEHSWGDGVAVLRFFNEVFRDSTQ	586	ILSTSILN.....SPAVSLGSGFAPVV
CPT2_MOUSE	131	FNPFMAFNP	368	VHFEHSWGDGVAVLRFFNEVFRDSTQ	586	ILSTSILS.....SPAVSLGSGFAPVV
CPT2_HUMAN	131	FNPFMAFNP	368	VHFEHSWGDGVAVLRFFNEVFKDSTQ	586	VLSTSILS.....SPAVNLGSGFAPVV
OCTC_RAT	101	VNPFVGPSPH	323	CSCDHAPYDAMLVNIHIAFVEKDLLE	540	VLSTSILV.....YLRVQGVVVVPMV
OCTC_HUMAN	101	VNFAGPAAH	323	CNCDHAPFDAMIMVNIISYYVDEKIFQ	540	VLSTSILV.....YLRVQGVVVVPMV
OCTC_BOVIN	101	VNFGGPASH	323	SNCDHAPFDAMVLVKVCYYVDENILE	540	VLSTSILV.....YLRVQGVVVVPMV
CACP_HUMAN	118	SSPGVMLPK	339	LVYEHAAAEGLP I VTLDDYVIEYTKK	550	HLSTSQVP.....AKTDCVMEFGPVV
CACP_MOUSE	118	SSPGVILPK	339	MVYEHAAAEGLP I VALVDHVMEYTKK	550	NLSTSQVP.....AKTDCVMEFGPVV
CACP_RAT	118	SSPGVLLPK	339	MVYEHAAAEGLP I VALVDHVMEYTKK	550	NLSTSQVP.....AKTDCVMEFGPVV
		EEEE		HHHHHHHH	EEEEEE	EEE
		E1		H12	E13	E14

FIG. 2. Alignment of representative sequences of mammalian carnitine-acyltransferases. Amino acid sequence of 17 representative enzymes that catalyze short acyl-CoAs as substrates: CrAT (CACP) from human, mouse, and rat; and enzymes which have medium- and long-chain acyl-CoAs as substrates: L-CPT I (CPT1) from rat, mouse, and human; M-CPT I (CPTM) from human, rat, and mouse; brain CPT I (CPTC) from human and mouse; CPT II (CPT2) from rat, mouse, and human; and COT (OCTC) from human, rat, and bovine; were obtained from the Swiss-Prot data bank and aligned using ClustalW. The subfamily conserved residue according to acyl-CoA chain-length specificity is shaded in black: for CrAT it is a methionine; and for COT, L-CPT I, M-CPT I, brain CPT I-c, and CPT II it is a glycine. Position of catalytic histidine, catalytic aspartic/glutamic, STS catalytic domain and a conserved proline residue, are also shaded in gray. Secondary structure elements are indicated as in Fig. 1.

hydrocarbon chain of acyl-CoA as substrate, and therefore we prepared CrAT mutant M564G, which we then expressed in the budding yeast, *S. cerevisiae*.

Enzyme activity of yeast-expressed CrAT mutant M564G was tested for acyl-CoA substrates of various lengths and compared with wt CrAT. Wild-type CrAT was highly active toward acetyl-CoA and butyryl-CoA (Fig. 3A), but not toward other, longer-chain acyl-CoAs. The activity was practically zero with dodecanoyl-CoA and longer acyl-CoAs. In contrast, CrAT mutant M564G (Fig. 3B) was more active toward longer acyl-CoAs: it showed a new activity toward palmitoyl-CoA and a 1250-fold increase of activity toward myristoyl-CoA (Tables I and II). This figure was calculated after determination of enzyme activities with highly purified wt CrAT after expression in *E. coli* (see "Experimental Procedures"). Otherwise, activity also increased with dodecanoyl- (58-fold), decanoyl- (7-fold), octanoyl- (11-fold), and hexanoyl-CoA (7-fold), while activity toward acetyl-CoA decreased 50%. These values indicate that the long side chain of methionine impedes the positioning of medium- and long-chain acyl-CoAs in the hydrophobic pocket, but when this side chain is shortened (as in the mutant) other, longer acyl-CoAs fit the catalytic site and catalysis proceeds.

**Kinetic Characteristics of wt CrAT and Mutant M564G**—A series of kinetic experiments were performed by varying the length of the acyl-CoA substrate (from C2 to C16 acyl-CoA) with both wt CrAT and mutant M564G. The mutant showed standard saturation kinetics for both carnitine and acyl-CoA substrates, as did the wt CrAT (data not shown). This property was general for every acyl-CoA, irrespective of its length.  $K_m$  values for wt CrAT varied slightly (between 23 and 33  $\mu\text{M}$ ) with the chain length of the substrate (Table I).  $V_{\max}$  was maximal for butyryl-CoA and then decreased for longer acyl-CoAs. Wild-type CrAT  $V_{\max}$  and catalytic efficiency (defined as  $V_{\max}/K_m$  ratio) for octanoyl-CoA was only 8% of those for acetyl-CoA.  $K_m$  and  $V_{\max}$  for carnitine as substrate were also measured by varying the length of acyl-CoA.  $K_m$  increased with the length of the acyl-CoA substrate.  $K_m$  for carnitine with octanoyl-CoA as substrate was 5-fold that for acetyl-CoA, and concomitantly,  $V_{\max}$  decreased to 10% when octanoyl-CoA was the substrate in comparison with acetyl-CoA. Catalytic efficiency for carnitine

also decreased; for example, catalytic efficiency for octanoyl-CoA was only 2% versus acetyl-CoA. This implies that short-chain acyl-CoAs are preferential substrates when the concentration of carnitine is low and that the binding of long acyl-CoAs lowers affinity for carnitine.

Different behavior was observed with CrAT mutant M564G (Table II). Although  $K_m$  values for fatty acyl-CoA varied slightly with the chain length (between 11 and 32  $\mu\text{M}$ ),  $V_{\max}$  increased, particularly with hexanoyl-CoA. Another maximum of activity was also observed with myristoyl-CoA.  $K_m$  for carnitine decreased when the acyl-CoA was long, showing that the mutant preferred long-chain acyl-CoAs as substrates. Catalytic efficiencies for both carnitine and acyl-CoA increased with the length of acyl-CoA, values for hexanoyl-CoA and octanoyl-CoA being the highest. In contrast to the wt CrAT, mutant M564G behaved as if its natural substrates were medium- and long-chain acyl-CoAs.

The comparison of catalytic efficiencies between octanoyl-CoA and acetyl-CoA for the wt and CrAT mutant M564G shows that this point mutation produced an increase of 103-fold. We did not compare catalytic efficiencies for longer fatty acyl-CoAs, because their activities were too low. These results were interpreted as showing that replacement of methionine by glycine increased the space for positioning of carnitine and acyl-CoA, which in turn increased the catalytic efficiency.

**Re-engineering COT Specificity**—Through the experiments performed above we had converted rat CrAT into a pseudo rat COT, which was able to catalyze medium- and long-chain acyl-CoAs. Our aim was then to achieve the opposite, that is, to transform rat COT into a pseudo rat CrAT by modifying a single amino acid. The catalytic activity of CrAT mutant M564G toward different acyl-CoAs was very similar to that of wt COT (Fig. 3, B and D). To improve our definition of the role of COT Gly<sup>553</sup> (orthologous to CrAT Met<sup>564</sup>) in catalytic activity with respect to acyl-CoAs of different lengths, COT mutant G553M was prepared and expressed in *S. cerevisiae*.

Enzyme activity of yeast-expressed COT mutant G553M was tested with substrates of different length and compared with wt COT (Fig. 3). Results show that wt COT was highly active toward medium-chain acyl-CoAs: hexanoyl-, octanoyl-, and dec-

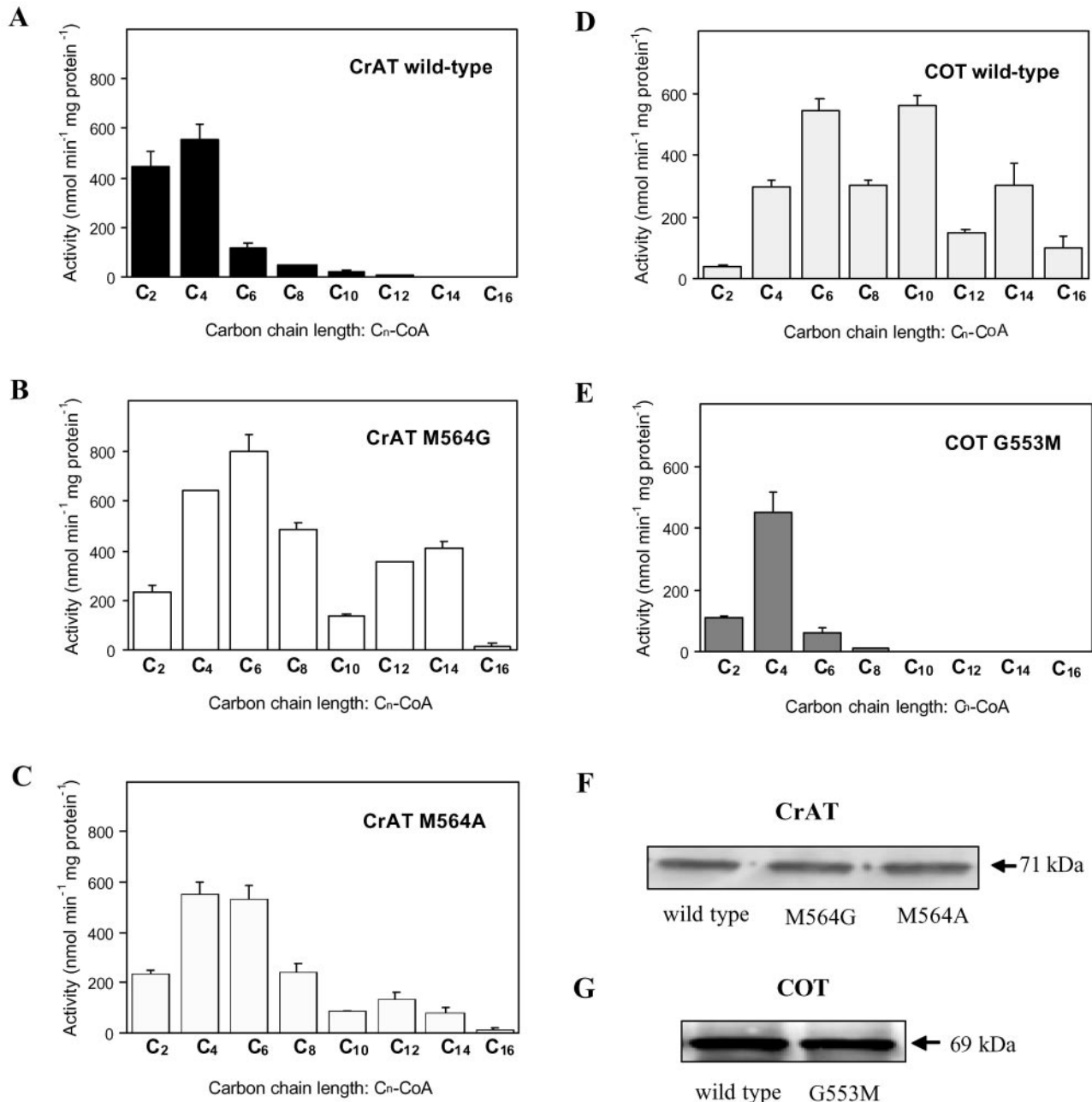


**FIG. 3. Carnitine acyltransferase activity of *S. cerevisiae* cells expressing wt CrAT and COT and the point mutants CrAT M564G, M564A, and COT G553M.** Extracts from yeast expressing wt CrAT (A), wt COT (D), and point mutants CrAT M564G (B), M564A (C), and COT G553M (E) were assayed for activity with acyl-CoAs of different chain length ranging from acetyl-CoA to palmitoyl-CoA, as described under "Experimental Procedures." The results are the mean  $\pm$  S.D. of at least three independent experiments with different preparations. Immunoblots showing expression of wt CrAT, CrAT M564G, and M564A (F); and of wt COT and COT G553M (G). *S. cerevisiae* extracts (8  $\mu$ g for CrAT and 10  $\mu$ g for COT) were separated by SDS-PAGE and subjected to immunoblotting using specific antibodies. The arrows indicate the migration position and the molecular mass of rat CrAT (71 kDa) and rat COT (69 kDa).

anoyl-CoA, but not toward other acyl-CoAs with either a shorter or a longer hydrocarbon chain. COT mutant G553M showed much lower activity toward medium- and long-chain acyl-CoAs, but a slight increase in activity toward short-chain acyl-CoAs (acetyl-, and butyryl-CoA), showing maximum activity toward butyryl-CoA: at variance with wt COT, but the same as wt CrAT (Fig. 3).

COT mutant G553M showed a 31-fold decrease in activity when octanoyl-CoA was the substrate with respect to wt COT. Activity with hexanoyl-CoA also decreased (9-fold). Activities of COT mutant G553M toward acyl-CoAs containing between 10 and 16 carbons in their chain were undetectable, so the profile of activities toward the whole list of acyl-CoAs was practically

identical to that of wt CrAT. Mutation of Gly<sup>553</sup> to Met in COT reproduced the substrate specificity of wt CrAT. Western blot of yeast-expressed wt and mutants CrAT and COT showed the same molecular masses and similar expression levels (Figs. 3, F and G).

**Positioning of Fatty Acyl-CoAs in the Wild-type and Mutated CrAT and COT Models**—A common model is proposed for the location of acyl-CoAs in the active center of both CrAT and COT enzymes (Fig. 4). Three-dimensional models of the rat wt CrAT and COT were generated by homology-modeling procedures using the crystallized structures of mouse and human CrAT as templates (14, 15), in a similar way to that used to construct the model for rat CPT I, as described elsewhere (34). The

TABLE I  
Enzyme activity and kinetic parameters of CrAT wt expressed in *S. cerevisiae*

Mitochondrial protein from yeast expressing wt CrAT were assayed with acyl-CoAs of different carbon lengths ranging from acetyl-CoA to palmitoyl-CoA, as described under "Experimental Procedures." The results are the mean  $\pm$  S.D. of at least three independent experiments with different preparations.

Acyl-CoA	Activity <i>nmol·min<sup>-1</sup>·mg protein<sup>-1</sup></i>	$K_m$		$V_{max}$		Catalytic efficiency	
		Carnitine	Acyl-CoA	Carnitine	Acyl-CoA	Carnitine	Acyl-CoA
		$\mu M$		<i>nmol·min<sup>-1</sup>·mg protein<sup>-1</sup></i>		$V_{max}/K_m$	
C <sub>2</sub> -CoA	442 $\pm$ 66	203 $\pm$ 21	22.8 $\pm$ 1.0	515 $\pm$ 56	550 $\pm$ 99	2.53	24.1
C <sub>4</sub> -CoA	553 $\pm$ 62	220 $\pm$ 54	30.7 $\pm$ 2.8	567 $\pm$ 97	685 $\pm$ 85	2.58	22.3
C <sub>6</sub> -CoA	119 $\pm$ 16	567 $\pm$ 80	33.2 $\pm$ 4.6	176 $\pm$ 22	148 $\pm$ 5.1	0.31	4.46
C <sub>8</sub> -CoA	45.7 $\pm$ 6.5	964 $\pm$ 120	24.7 $\pm$ 6.5	53 $\pm$ 8.0	45.0 $\pm$ 7.1	0.05	1.82
C <sub>10</sub> -CoA	20.3 $\pm$ 4.1	ND <sup>a</sup>	ND	ND	ND	ND	ND
C <sub>12</sub> -CoA	6.0 $\pm$ 2.6	ND	ND	ND	ND	ND	ND
C <sub>14</sub> -CoA	0.33 $\pm$ 0.07 <sup>b</sup>						
C <sub>16</sub> -CoA	UD <sup>c</sup>						

<sup>a</sup> ND, not determined.

<sup>b</sup> This activity was obtained using purified rat CrAT expressed in *E. coli*.

<sup>c</sup> UD, undetectable activity.

TABLE II  
Enzyme activity and kinetic parameters of CrAT mutant M564G in *S. cerevisiae*

Mitochondrial protein from yeast expressing CrAT mutant M564G were assayed with acyl-CoAs of different carbon length ranging from acetyl-CoA to palmitoyl-CoA, as described under "Experimental Procedures." The results are the mean  $\pm$  S.D. of at least three independent experiments with different preparations.

Acyl-CoA	Activity <i>nmol·min<sup>-1</sup>·mg protein<sup>-1</sup></i>	$K_m$		$V_{max}$		Catalytic efficiency	
		Carnitine	Acyl-CoA	Carnitine	Acyl-CoA	Carnitine	Acyl-CoA
		$\mu M$		<i>nmol·min<sup>-1</sup>·mg protein<sup>-1</sup></i>		$V_{max}/K_m$	
C <sub>2</sub> -CoA	234 $\pm$ 30	339 $\pm$ 44	31.7 $\pm$ 5.3	197 $\pm$ 20.8	243 $\pm$ 25	0.58	7.7
C <sub>4</sub> -CoA	641 $\pm$ 3.2	170 $\pm$ 45	14.8 $\pm$ 1.0	742 $\pm$ 133	872 $\pm$ 125	4.4	59
C <sub>6</sub> -CoA	802 $\pm$ 66	164 $\pm$ 11	22.3 $\pm$ 6.0	1145 $\pm$ 255	1120 $\pm$ 106	7.0	50
C <sub>8</sub> -CoA	488 $\pm$ 24	86.0 $\pm$ 6.1	10.9 $\pm$ 3.6	522 $\pm$ 106	653 $\pm$ 110	6.1	60
C <sub>10</sub> -CoA	136 $\pm$ 7.3	26.9 $\pm$ 6.9	10.8 $\pm$ 1.7	153 $\pm$ 10.6	257 $\pm$ 41.6	5.7	24
C <sub>12</sub> -CoA	350 $\pm$ 0.5	ND <sup>a</sup>	ND	ND	ND	ND	ND
C <sub>14</sub> -CoA	409 $\pm$ 29	309 $\pm$ 50	12.7 $\pm$ 2.5	562 $\pm$ 84.6	505 $\pm$ 83.5	1.9	40
C <sub>16</sub> -CoA	18.1 $\pm$ 5.9	ND	ND	ND	ND	ND	ND

<sup>a</sup> ND, not determined.

models for the mutants CrAT M564G and COT G553M were built using the structural models of their respective wt enzymes as templates to ensure minimal variation in the atomic position of the residues located close to the active center of both proteins. The carnitine molecule and the CoA part of the acyl-CoAs were located using the information available in the crystallized structures of mouse CrAT (PDB entries: 1NDF and 1NDI (14)). Positioning of the acyl part of the acetyl-, decanoyl-, and myristoyl-CoA substrates was modeled by the simulation docking algorithms Autodock (27, 28) and Hex (29).

The location of acetyl-CoA in the active center of the model for rat wt CrAT (Fig. 4A) is, as expected, very similar to that described for CoA in the crystallized mouse CrAT. The sulfur atom of the CoA molecule is close to carnitine and to the catalytic His<sup>343</sup>, whereas the acetyl group appears to lie in a small cavity defined, by the  $\beta$ -sheets E1, E13, and E14, as the walls of the hollow, and by the lateral chain of residue Met<sup>564</sup> as the floor. Surprisingly, the shape of the cavity appears to be very different in the structure of the active center of CrAT mutant M564G (Fig. 4B). The small size of the side chain of Gly<sup>564</sup> reveals a deeper pocket in the same position as the shallow cavity in the wt molecule. This preformed pocket is now accessible to longer acyl groups, as can be modeled using myristoyl-CoA as substrate. The position of the fatty acyl part of myristoyl-CoA is very similar to that modeled for the palmitoyl part of palmitoyl-CoA in a hydrophobic pocket of CPT I (34). The open cavity of CrAT mutant M564G is surrounded by Gly<sup>564</sup>, by hydrophobic residues Val<sup>122</sup>, Leu<sup>124</sup>, Ile<sup>351</sup>, Val<sup>352</sup>, Val<sup>355</sup>, Met<sup>359</sup>, Val<sup>556</sup>, Ala<sup>558</sup>, and Cys<sup>562</sup> (located in  $\beta$ -sheets E1, E13, and E14 and in  $\alpha$ -helix H12, as in CPT I) and by polar residues Asp<sup>356</sup> and Thr<sup>560</sup> at the bottom. Interestingly, it

appears that the cavity for longer acyl groups is preformed in CrAT and that Met<sup>564</sup> acts as a lid to close the access to the hydrophobic pocket (Fig. 5A). When the side chain of Met<sup>564</sup> is removed, the pocket is now accessible, extending the sensitivity of the enzyme to long-chain acyl-CoA substrates (Fig. 5B). This is consistent with the enzymatic activity observed when using C8, C10, C12, and C14 acyl-CoA as substrates (Fig. 3B).

The model for wt COT and its interaction with decanoyl-CoA is very similar to the one for CrAT mutant M564G and myristoyl-CoA. The sulfur atom of the acyl-CoA molecule is close to carnitine and to His<sup>327</sup>, the catalytic residue, whereas the fatty acid extension is enclosed in a pocket (Fig. 4C) defined by the side chain of hydrophobic residues positioned in  $\beta$ -sheets E1, E13, and E14 and in  $\alpha$ -helix H12: Val<sup>104</sup>, Ala<sup>332</sup>, Met<sup>333</sup>, Met<sup>335</sup>, Val<sup>336</sup>, Ala<sup>339</sup>, Leu<sup>545</sup>, Leu<sup>549</sup>, and Ile<sup>551</sup>. The floor of the cavity is occupied by polar residues Ser<sup>107</sup> and Asp<sup>343</sup>. In contrast, the structure for COT mutant G553M resembles that for wt CrAT: the side chain of Met<sup>553</sup> now closes the entrance to the pocket and defines a narrow cavity, structurally equivalent to that of the active center in wt CrAT, where the small acetyl group of acetyl-CoA can be fitted (Fig. 4D). In symmetry with CrAT, the hydrophobic cavity for long acyl-CoAs in the COT structure can be closed by the lateral chain of Met<sup>553</sup>, which acts as a lid, like the corresponding residue in CrAT, Met<sup>564</sup>. The model again correlates with the enzymatic activities of wt and mutant COT when using short- and long-chain acyl-CoAs as substrates (Fig. 3).

*The Mutant M564A Also Broadened the Specificity of CrAT*—Because glycine does not constrain the backbone psi/phi angles, its substitution for methionine could modify substrate specificity simply as a result of increased flexibility. To rule out this

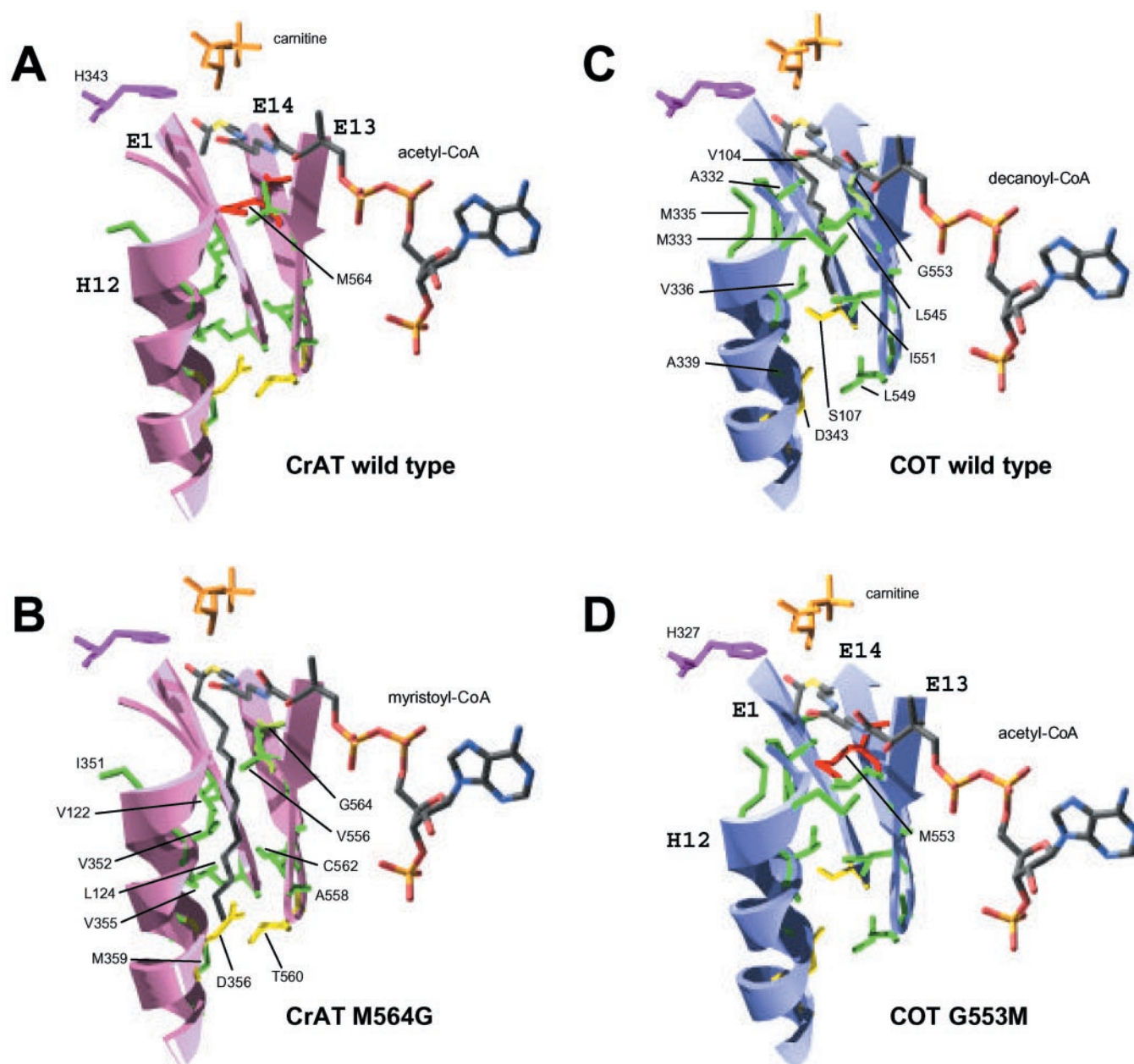


**FIG. 4. Proposed models for the positioning of fatty acyl-CoAs in the wt and mutated CrAT and COT.** *A*, location of a molecule of acetyl-CoA in the active center of wt CrAT. Position of Met<sup>564</sup> (red) as well as the secondary structure elements alpha helix 12 and beta strands 1, 13, and 14, surrounding the acetyl hollow, are indicated. The molecule of carnitine, as well as the catalytic residue His<sup>343</sup> are also represented. *B*, location of a molecule of myristoyl-CoA in the deep pocket opened in the CrAT mutant M564G. Positions of Gly<sup>564</sup>, hydrophobic residues around the acyl-chain (Val<sup>122</sup>, Leu<sup>124</sup>, Ile<sup>351</sup>, Val<sup>352</sup>, Val<sup>355</sup>, Met<sup>359</sup>, Val<sup>556</sup>, Ala<sup>558</sup>, and Cys<sup>562</sup>) and polar residues Asp<sup>356</sup> and Thr<sup>560</sup> are indicated. *C*, a molecule of decanoyl-CoA in the hydrophobic pocket defined by alpha helix 12 and beta strands 1, 13, and 14 of wt COT. Positions of Val<sup>104</sup>, Ala<sup>332</sup>, Met<sup>333</sup>, Met<sup>335</sup>, Val<sup>336</sup>, Ala<sup>339</sup>, Leu<sup>545</sup>, Leu<sup>549</sup>, and Ile<sup>551</sup> and the polar residues Ser<sup>107</sup> and Asp<sup>343</sup> are indicated. *D*, model for the location of a molecule of acetyl-CoA in the shallow cavity closed by Met<sup>553</sup> (red) of COT mutant G553M. Carnitine, His<sup>327</sup>, and the positions of secondary structure elements helix 12 and beta strands 1, 13, and 14 are also represented.

possibility, we prepared another CrAT mutant, M564A. Alanine is also a small amino acid, but, unlike glycine, it does not affect flexibility. So if methionine/glycine acts as a molecular gate to prevent/permit acyl-CoA binding as a function of chain length, the alanine mutant should behave similarly to the glycine. The change of specificity of the alanine mutant might not be as pronounced, but it would still be able to catalyze acyl-CoAs longer than acetyl-CoA and butyryl-CoA.

Accordingly, we expressed the CrAT mutant M564A in *S. cerevisiae*, and the extracts were assayed for carnitine acyltransferase activity using acyl-CoAs of various chain lengths as substrates. The results were similar to those found in mutant M564G, (Fig. 3C). For instance, CrAT mutant M564A activity

toward myristoyl-CoA increased 242-fold with respect to the wt CrAT. The -fold activation of the M564A mutant toward acyl-CoAs of between C6 and C12 ranged between 5- and 23-fold. CrAT M564A also showed some activity toward palmitoyl-CoA (11 nmol·min<sup>-1</sup>·mg protein<sup>-1</sup>), which was absent in wt CrAT. In addition, the activity of CrAT mutant M564A toward its natural substrate acetyl-CoA was less than half that of wt CrAT.

**Activity of CrAT Mutants H343A and E347A**—It is generally accepted that a histidine is the main catalytic residue in carnitine acyltransferases. This critical histidine residue had been mutated in several proteins of the carnitine acyltransferase family like rat CPT II (16), rat L-CPT-I (18), rat COT (19), and

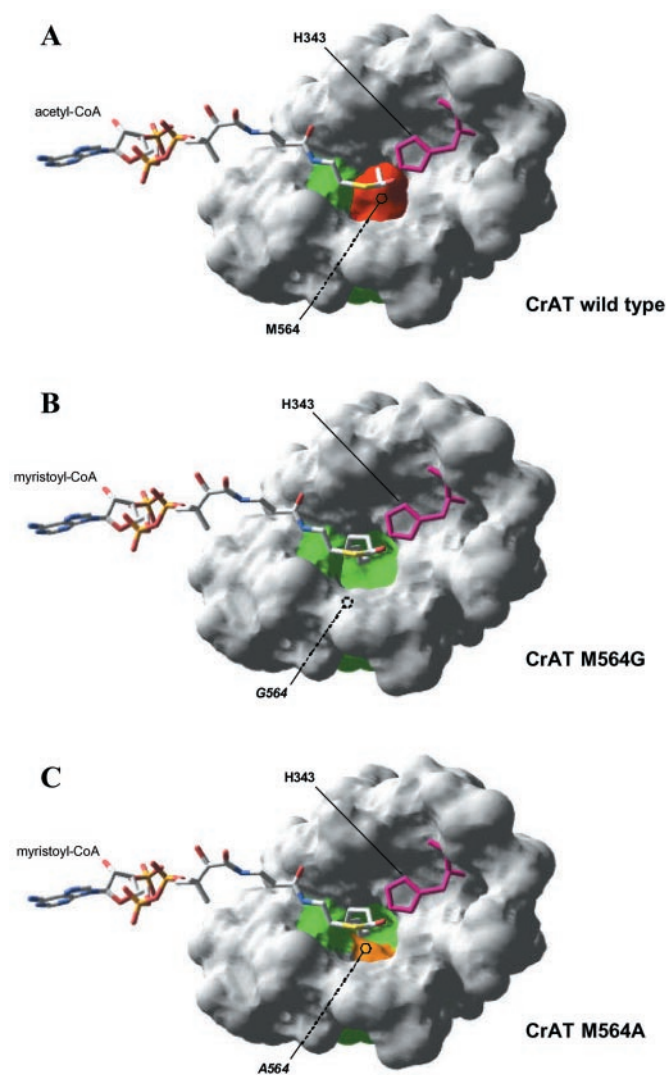


FIG. 5. **Substrate docking in wt CrAT and mutants.** Proposed location of acetyl-CoA and myristoyl-CoA acyl-chains in the active centers of rat CrAT wt (A), mutant M564G (B), and mutant M564A (C) surface structural models, respectively. Hydrophobic residues in the walls of the deep pocket are colored in green. Met<sup>564</sup> surface, closing the cavity in wild-type CrAT, is depicted in red. Ala<sup>564</sup> is depicted in yellow. Catalytic His<sup>343</sup> is also represented (pink trace).

human peroxisomal CrAT (15), and in all cases the mutation completely abolished enzyme activity. To see whether the homologous histidine behaved similarly in rat CrAT, we mutated CrAT His<sup>343</sup> to Ala, because this position is orthologous to other carnitine acyltransferases. Enzyme activity of CrAT mutant H343A was abolished.

We also mutated Glu<sup>347</sup> to Ala in rat CrAT. In almost all the other members of the family, an aspartate is found at this position, which could functionally be substituted for glutamate. The mutation of the Glu<sup>347</sup> to Ala resulted in total loss of catalytic activity.

Both CrAT mutants H343A and E347A were expressed in *S. cerevisiae* at similar levels to the wt (data not shown), on the basis of which the hypothesis that the abolition of activity was caused by low protein expression was ruled out.

#### DISCUSSION

Previous to this study, an mRNA sequence of rat CrAT had been reported, based on the *in silico* localization of several open reading frames (accession number XM\_242301) observed in the genomic rat CrAT sequence (accession number NW\_047651).

The genomic organization of the postulated rat CrAT was similar to CrATs from various organisms (35). However, it was also postulated to contain an extra exon (exon 7bis) not found in any other organism, solely on the basis of the observation of an open reading frame of 81 nt within intron 7. Our findings after sequencing the rat CrAT cDNA did not reveal the proposed exon 7bis. To establish whether this exon is present in mature CrAT mRNA, a shorter cDNA fragment comprising the putative exon 7bis was PCR-amplified. No such sequence was found, from which it was concluded that rat CrAT does not contain an exon 7bis. Nor was such an exon observed in any published CrAT cDNA sequence or in 40 published expressed sequence tag sequences from rat CrAT, and no such amino acid sequence can be aligned with protein sequences of CPT I, CPT II, or COT from various organisms. Alternatively, if such an exon were to exist, rat testis expression of the processed mRNA containing exon 7bis would be undetectable even using PCR amplification.

The use of a mutant strain of *S. cerevisiae* devoid of CrAT and COT activity allowed us to express wt and mutant rat CrAT and COT cDNAs and study their kinetic characteristics. The results show that the yeast-expressed CrAT behaves like rat CrAT from mitochondria (36). This is the first time that mammalian CrAT has been expressed in yeast.

The carnitine acyltransferases family has a common catalytic mechanism, which is the transfer of the fatty acid moiety from fatty acyl-CoA to carnitine in a process that involves deprotonation of carnitine and nucleophilic attack of the carbonyl carbon of the thioester bond of acyl-CoA. In CrAT the residue implicated in this process is His<sup>343</sup>. Mutant H343A was expressed in *S. cerevisiae*, and the activity of the mutant was abolished, although the expression was practically identical to wt CrAT. Other carnitine acyltransferases stabilize the catalytic histidine through an aspartic acid. Glu<sup>347</sup> occupies the same position in CrAT as an aspartic residue in other carnitine acyltransferases (34). The important role of Glu<sup>347</sup> in CrAT activity is clearly defined, because mutant E347A abolished enzyme activity, as seen in CPT II (16).

This general mechanism, which also corresponds to a similar three-dimensional structure (34), is nevertheless complemented by substrate-specific characteristics. Substrate specificity is now well defined, on the basis of the studies of various groups: CrAT catalyzes short-chain acyl-CoAs (acetyl-CoA, propionyl-CoA, and butyryl-CoA) (36–39), whereas COT catalyzes medium-chain acyl-CoAs containing between 6 and 12 carbons (40, 41), and CPT I and CPT II catalyze palmitoyl-CoA and long-chain fatty acyl-CoAs (40). We hypothesized that a structural feature on the enzyme might be responsible for substrate specificity, depending the length of the acyl-CoAs. We addressed this question with CrAT and COT.

The putative amino acid residue responsible for governing the access of the acyl-CoA was identified by close examination of the catalytic site in CrAT crystals. The recent report of the crystal structure of mouse (14) and human CrAT (15) suggested Met<sup>564</sup> as a candidate, because its side chain is voluminous and projects into the putative cavity where the acyl-CoA may enter. The fact that methionine is a bulky residue suggests a possible role in permitting the access of only short-chain substrates such as acetyl-CoA and butyryl-CoA. Interestingly, according to the information gleaned from multiple alignment of the sequences of the carnitine acyltransferases family of proteins, the presence of either a Gly or a Met residue in the same position is, respectively, a common feature in all long-chain and short-chain acyl-CoA enzymes. This type of position, in multiple alignment with a pattern of variation related to differences in function of the corresponding groups of subfamilies of pro-



teins, implies functional and structural changes that are selected through evolution. Such residues are conceptually related with specific active sites, substrate binding sites, or inhibitor interaction patches (42), as demonstrated in the case of the interaction of several members of the carnitine acyltransferases family with the inhibitor malonyl-CoA (43).

**Mutation of Met<sup>564</sup> to Glycine Opens the Hydrophobic Pocket to Medium- and Long-chain Acyl-CoAs**—By alignment we identified the orthologous amino acid Met<sup>564</sup> residue in carnitine acyltransferases that catalyze substrates of longer chain than acetyl-CoA. It was clear that not only COT but also CPT I and CPT II contain a glycine in this position (Fig. 2). This suggested that the smaller glycine was probably the residue that allows free access of the long-chain fatty acyl-CoAs, whereas the larger side chain of Met<sup>564</sup> prevented the access of long-chain acyl-CoAs. CrAT mutant M564G produced positive results that vindicate these expectations.

The increases in activity and catalytic efficiency toward long-chain acyl-CoAs in the CrAT mutant M564G were not accompanied by changes in  $K_m$  for acyl-CoA. Maximal changes were observed in  $V_{max}$  and catalytic efficiency, which suggests that these increases in catalytic activity are attributable to the altered accessibility of the catalytic site.

The Michaelis constants for substrates ranging from acetyl-CoA to octanoyl-CoA are very similar (Table I). This poses the question as to whether the various acyl-CoAs in the wt model are located in the hydrophobic pocket or in the catalytic channel. If the latter were the case, acyl-CoAs would displace carnitine from its site. This appears to occur, as carnitine  $K_m$  increases when the chain length of acyl-CoA increases. Carnitine is presumably displaced, and catalysis is prevented, as indicated by the low  $V_{max}$  of the wt CrAT in the presence of long-chain acyl-CoAs. If the hydrophobic pocket is open, as shown in the CrAT mutant M564G, the long hydrocarbon chain can occupy it. Consequently, carnitine  $K_m$  decreases when long-chain acyl-CoAs increase (except for myristoyl-CoA) and catalytic efficiencies for medium and long-chain acyl-CoA increase, and catalysis proceeds.

**Mutation of COT Gly<sup>553</sup> to Methionine Closes the Hydrophobic Pocket**—These hypotheses were confirmed by the reverse experiment: we mutated COT Gly<sup>553</sup> to methionine, and the new mutant behaved like wt CrAT. Results of COT mutant G553M activity in relation with the acyl-CoA used as substrate are very similar to those of wt CrAT. The same applies to CrAT mutant M564G and wt COT: the pattern of activities in relation to acyl-CoAs of different lengths is very similar. In both cases the enzymes containing glycine rather than methionine (CrAT mutant M564G and wt COT) present high enzyme activities with medium and long chain fatty acyl-CoAs, whereas their activity toward acetyl-CoA is low.

An alternative explanation to the model of methionine/glycine acting as a gate to permit the location of longer acyl-CoAs could be based on increased flexibility of the mutant form, because glycine does not constrain the backbone psi/phi angles. Methionine, a larger residue, would render a more rigid environment, which would limit substrate binding. To discern between these two models, an intermediate situation was tested in which the Met<sup>564</sup> residue in CrAT was substituted by alanine (Fig. 5C). The presence of a methyl group in the side chain of alanine would mimic the presence of the methionine in terms of backbone flexibility (reducing the degrees of freedom of the phi/psi angles of the backbone), but, in contrast, it would also reflect the small size of the glycine residue. The results obtained in these new conditions, which were similar to those obtained in the Gly mutant, strongly support the gate model. This can be taken as a demonstration that a single mutant is

able to switch the substrate specificity of CrAT and COT. Kinetic data together with information obtained from the three-dimensional models of wt or CrAT and COT mutants indicate that CrAT Met<sup>564</sup> and its orthologous COT Gly<sup>553</sup> are the residues responsible for the substrate specificity of these enzymes.

Wild type CrAT and COT have 32% amino acid sequence identity and, accordingly, the pattern of activity of the two enzymes toward acyl-CoAs of various lengths is very different. It is noteworthy that CrAT mutant M564G retains the same sequence identity with wt COT; however, the substrate specificity of this mutant is practically identical to that of wt COT. The same argument applies to COT; COT mutant G553M shares 32% identity with wt CrAT; however, its substrate specificity is practically identical to wt CrAT. These figures confirm that Met<sup>564</sup> is the amino acid responsible for the acyl-CoA specificity. Despite the fact that 68% of the amino acids are different in mutant CrAT and wt COT, the change of only one critical amino acid has rendered both proteins practically identical in terms of substrate specificity.

To our knowledge, this is the first study to show that mutation of a single amino acid leads to such dramatic modification of specificity in the various enzymes that use acyl-CoAs of various lengths. Studies carried out in acyl-CoA dehydrogenase (44, 45) show that a small change in specificity is obtained after mutation of three residues or more. Mutation of one residue slightly modified substrate specificity in the hydrolysis of esters from *Burkholderia cepacia*, and the combined action of two mutations increased the specificity to *p*-nitrophenyl palmitate by about 5-fold (46). Analogous results were obtained with *Candida rugosa* lipase, in which mutation L304F led to a 3-fold increase in the hydrolysis of a randomized oil *versus* wt enzyme (47).

The hydrophobic pocket of CrAT described in this study is the same as the one we proposed for CPT I (34). In that case, the orthologous glycine, which allows correct positioning of acyl-CoA, is surrounded by two other glycines conforming a gap that is wide enough to allow the entry of the hydrocarbon chain into the cavity before catalysis.

In summary, for the first time we have identified an amino acid residue that is critical to fatty acyl chain-length specificity in CrAT. This study may enhance our understanding of the structure-function relationship for other carnitine acyltransferases within the context of fatty acid metabolism.

**Acknowledgment**—We thank Robin Rycroft of the Language Service for valuable assistance in the preparation of the English manuscript.

#### REFERENCES

- McGarry, J. D., and Brown, N. F. (1997) *Eur. J. Biochem.* **244**, 1–14
- Esser, V., Britton, C. H., Weis, B. C., Foster, D. W., and McGarry, J. D. (1993) *J. Biol. Chem.* **268**, 5817–5822
- Yamazaki, N., Shinohara, Y., Shima, A., and Terada, H. (1995) *FEBS Lett.* **363**, 41–45
- Price, N. T., van der Leij, F. R., Jackson, V. N., Corstorphine, C. G., Thomson, R., Sorensen, A., and Zammit, V. A. (2002) *Genomics* **80**, 433–442
- Bieber, L. L., Krahling, J. B., Clarke, P. R., Valkner, K. J., and Tolbert, N. E. (1981) *Arch. Biochem. Biophys.* **211**, 599–604
- Bieber, L. L. (1988) *Annu. Rev. Biochem.* **57**, 261–283
- Zammit, V. A. (1999) *Prog. Lipid. Res.* **38**, 199–224
- Brunner, S., Kramar, K., Denhardt, D. T., and Hofbauer, R. (1997) *Biochem. J.* **322**, 403–410
- Kalaria, R. N., and Harik, S. I. (1992) *Ann. Neurol.* **32**, 583–586
- Makar, T. K., Cooper, A. J., Tofel-Grehl, B., Thaler, H. T., and Blass, J. P. (1995) *Neurochem. Res.* **20**, 705–711
- DiDonato, S., Rimoldi, M., Moise, A., Bertagnoglio, B., and Uziel, G. (1979) *Neurology* **29**, 1578–1583
- Brevetti, G., Angelini, C., Rosa, M., Carrozzo, R., Perna, S., Corsi, M., Marazzato, A., and Marcialis, A. (1991) *Circulation* **84**, 1490–1495
- Meleg, B., Seress, L., Bedekovics, T., Kispal, G., Sümegi, B., Trombitas, K., and Mehes, K. (1999) *J. Inher. Metab. Dis.* **22**, 827–838
- Jogl, G., and Tong, L. (2003) *Cell* **112**, 113–122
- Wu, D., Govindasamy, L., Lian, W., Gu, Y., Kukar, T., Agbandje-McKenna, M., and McKenna, R. (2003) *J. Biol. Chem.* **278**, 13159–13165
- Brown, N. F., Anderson, R. C., Caplan, S. L., Foster, D. W., and McGarry, J. D.

- (1994) *J. Biol. Chem.* **269**, 19157–19162
17. Govindasamy, L., Kukar, T., Lian, W., Pedersen, B., Gu, Y., Agbandje-McKenna, M., Jin, S., McKenna, R., and Wu, D. (2004) *J. Struct. Biol.* **146**, 416–424
18. Morillas, M., Gómez-Puertas, P., Roca, R., Serra, D., Asins, G., Valencia, A., and Hegardt, F. G. (2001) *J. Biol. Chem.* **276**, 45001–45008
19. Morillas, M., Clotet, J., Rubí, B., Serra, D., Asins, G., Ariño, J., and Hegardt, F. G. (2000) *FEBS Lett.* **466**, 183–186
20. Guex, N., and Peitsch, M. C. (1997) *Electrophoresis* **18**, 2714–2723
21. Guex, N., Diemand, A., and Peitsch, M. C. (1999) *Trends. Biochem. Sci.* **24**, 364–367
22. Peitsch, M. C. (1995) *Bio/Technology* **13**, 658–660
23. Peitsch, M. C. (1996) *Biochem. Soc. Trans.* **24**, 274–279
24. Hooft, R. W. W., Vriend, G., Sander, C., and Abola, E. E. (1996) *Nature* **381**, 272
25. Vriend, G. (1990) *J. Mol. Graph.* **8**, 52–56
26. Laskowski, R. A., MacArthur, M. W., Moss, D. S., and Thornton, J. M. (1993) *J. Appl. Cryst.* **26**, 283–291
27. Goodsell, D. S., Morris, G. M., and Olson, A. J. (1996) *J. Mol. Recognit.* **9**, 1–5
28. Morris, G. M., Goodsell, D. S., Halliday, R. S., Huey, R., Hart, E., Belew, R. K., and Olson, A. J. (1998) *J. Comput. Chem.* **19**, 1639–1662
29. Ritchie, D. W., and Kemp, G. J. (2000) *Proteins* **39**, 178–194
30. Swiegers, J. H., Dippenaar, N., Pretorius, I. S., and Bauer, F. F. (2001) *Yeast* **18**, 585–595
31. Hassett, R. P., Crockett, E. L. (2000) *Anal. Biochem.* **287**, 176–179
32. Corti, O., DiDonato, S., and Finocchiaro, G. (1994) *Biochem. J.* **303**, 37–41
33. Von Heijne, G. (1986) *EMBO J.* **5**, 1335–1342
34. Morillas, M., López-Viñas, E., Valencia, A., Serra, D., Gómez-Puertas, P., Hegardt, F. G., and Asins, G. (2004) *Biochem. J.* **379**, 777–784
35. van der Leij, F. R., Huijckman, N. C. A., Boomsma, C., Kuipers, J. R. G., and Bartelds, B. (2000) *Mol. Genet. Metab.* **71**, 139–153
36. Miyazawa, S., Ozasa, H., Furuta, S., Osumi, T., and Hashimoto, T. (1983) *J. Biochem.* **93**, 439–451
37. Chase, J. F. A. (1967) *Biochem. J.* **104**, 510–518
38. Bloisi, W., Colombo, I., Garavaglia, B., Giardini, R., Finocchiaro, G., and Didonato, S. (1990) *Eur. J. Biochem.* **189**, 539–546
39. Colucci, W. J., Gandour, R. D. (1988) *Bioorganic. Chem.* **16**, 307–334
40. Miyazawa, S., Ozasa, H., Osumi, T., and Hashimoto, T. (1983) *J. Biochem.* **94**, 529–542
41. Farrell, S. O., Fiol, C. J., Reddy, J. K., and Bieber, L. L. (1984) *J. Biol. Chem.* **259**, 13089–13095
42. López-Romero, P., Gómez, M. J., Gómez-Puertas, P., and Valencia, A. (2004) in *Principles and Practice. Methods in Proteome and Protein Analysis* (Kamp, R. M., Calvete, J., and Choli-Papadopoulou, T., eds) pp. 62–82, Springer-Verlag, Berlin
43. Morillas, M., Gómez-Puertas, P., Bentebibel, A., Selles, E., Casals, N., Valencia, A., Hegardt, F. G., Asins, G., and Serra, D. (2003) *J. Biol. Chem.* **278**, 9058–9063
44. He, M., Burghardt, T. P., and Vockley, J. (2003) *J. Biol. Chem.* **278**, 37974–37986
45. Souri, M., Aoyama, T., Yamaguchi, S., and Hashimoto, T. (1998) *Eur. J. Biochem.* **257**, 592–598
46. Yang, J., Koga, Y., Nakano, H., and Yamane, T. (2002) *Prot. Eng. Des. Sel.* **15**, 147–152
47. Schmitt, J., Brocca, S., Schmid, R. D., and Pleiss, J. (2002) *Prot. Eng. Des. Sel.* **15**, 595–601